Journal Pre-proof

Measurement of Adenovirus-Based Vector Heterogeneity

John M. Hickey , Shaleem I. Jacob , Andrew S. Tait , Fatemeh Dastjerdi Vahid , Joseph Barritt , Sarah Rouse , Alexander Douglas , Sangeeta B. Joshi , David B. Volkin , Daniel G. Bracewell

PII: S0022-3549(22)00578-0
DOI: https://doi.org/10.1016/j.xphs.2022.12.012
Reference: XPHS 2961

To appear in: *Journal of Pharmaceutical Sciences*

Received date: 12 October 2022
Revised date: 14 December 2022
Accepted date: 14 December 2022

Please cite this article as: John M. Hickey , Shaleem I. Jacob , Andrew S. Tait , Fatemeh Dastjerdi Vahid , Joseph Barritt , Sarah Rouse , Alexander Douglas , Sangeeta B. Joshi , David B. Volkin , Daniel G. Bracewell , Measurement of Adenovirus-Based Vector Heterogeneity, *Journal of Pharmaceutical Sciences* (2022), doi: https://doi.org/10.1016/j.xphs.2022.12.012

This is a PDF file of an article that has undergone enhancements after acceptance, such as the addition of a cover page and metadata, and formatting for readability, but it is not yet the definitive version of record. This version will undergo additional copyediting, typesetting and review before it is published in its final form, but we are providing this version to give early visibility of the article. Please note that, during the production process, errors may be discovered which could affect the content, and all legal disclaimers that apply to the journal pertain.

© 2022 Published by Elsevier Inc. on behalf of American Pharmacists Association.

Journal Pre-proof

Measurement of Adenovirus-Based Vector Heterogeneity

John M. Hickey[2¥], Shaleem I. Jacob[1¥], Andrew S. Tait[1¥], Fatemeh Dastjerdi Vahid[1], Joseph Barritt[3], Sarah Rouse[3], Alexander Douglas[4], Sangeeta B. Joshi[2], David B. Volkin[2], and Daniel G. Bracewell[1]*

[1] Department of Biochemical Engineering, University College London, London, UK

[2] Department of Pharmaceutical Chemistry, Vaccine Analytics and Formulation Center, University of Kansas, Lawrence, KS 66047, USA

[3] Department of Life Sciences, Imperial College London, London, UK

[4] Nuffield Department of Medicine, University of Oxford, Oxford, UK

[¥] JMH, SIJ and AST contributed equally to this work

* Correspondence to Prof. Daniel G. Bracewell: Biochemical Engineering, University College London, Gower Street, WC1E 6BT, London, United Kingdom Email: d.bracewell@ucl.ac.uk; Phone: +44 (0) 20 7679 9580;

Running Title: Analytical Characterization of ChAdOx1 and Ad5 heterogeneity

Key Words: Mass Spectrometry, Analytical Characterization, Transmission Electron Microscopy, Critical Quality Attributes, Adenovirus-based Vaccine, In-process testing

Journal Pre-proof

Journal Pre-proof

Abstract

Adenovirus vectors have become an important class of vaccines with the recent approval of Ebola and COVID-19 products. In-process quality attribute data collected during Adenovirus vector manufacturing has focused on particle concentration and infectivity ratios (based on viral genome: cell-based infectivity), and data suggest only a fraction of viral particles present in the final vaccine product are efficacious. To better understand this product heterogeneity, lab-scale preparations of two Adenovirus viral vectors, (Chimpanzee adenovirus (ChAdOx1) and Human adenovirus Type 5 (Ad5), were studied using transmission electron microscopy (TEM). Different adenovirus morphologies were characterized, and the proportion of empty and full viral particles were quantified. These proportions showed a qualitative correlation with the sample's infectivity values. Liquid chromatography-mass spectrometry (LC-MS) peptide mapping was used to identify key adenovirus proteins involved in viral maturation. Using peptide abundance analysis, a ~5-fold change in L1 52/55k abundance was observed between low- (empty) and high-density (full) fractions taken from CsCl ultracentrifugation preparations of ChAdOx1 virus. The L1 52/55k viral protein is associated with DNA packaging and is cleaved during viral maturation, so it may be a marker for infective particles. TEM and LC-MS peptide mapping are promising higher-resolution analytical characterization tools to help differentiate between relative proportions of empty, non-infectious, and infectious viral particles as part of Adenovirus vector in-process monitoring, and these results are an encouraging initial step to better differentiate between the different product-related impurities.

Journal Pre-proof

Abbreviations

LDF:	Low Density Fraction
HDF:	High Density Fraction
LC-MS:	Liquid Chromatography Mass Spectrometry
DTT:	Dithiothreitol
IAM:	Iodoacetamide
Ad5:	Human Adenovirus serotype 5
ChAdOx1:	Chimpanzee Adenovirus Oxford serotype Y25
CID:	Collision Induced Dissociation
CSH:	Charged Surface Hybrid
TEM:	Transmission Electron Microscopy
TFF:	Tangential Flow Filtration
AEX:	Anion Exchange Chromatography
P:I Ratio:	Ratio of the Number of Viral Particles to the Number of Infectious Viral Particles

Journal Pre-proof

Journal Pre-proof

Introduction

Adenoviral vectors have many therapeutic and prophylactic uses[1] including commercial gene therapy products and vaccines [2]. They are a significant class of viral vector because they can deliver large nucleic acid payloads (8-36 kbp)[3], therefore can offer treatment that require delivery of a large transposon payload into a target genome. Adenoviruses were the first DNA virus to enter rigorous therapeutic development, because of its well-defined biology, its genetic stability, its high gene transduction efficiency and its relative ease of large-scale production. [4] They are appealing vaccine candidates due to their long shelf life , which can be prolonged further with different additives and formulation strategies [5,6-,7].

There are many assays and techniques available to characterize different structural attributes of adenoviruses in accordance with regulatory guidelines [8-10]. Current quality control assays for viral vector-based vaccines comprise of a suite of: particle count by PCR, particle to infectivity ratio (determined by cell-based infectivity assays), residual host cell DNA and residual host cell protein[9]. In this work, we evaluated the potential utility of higher resolution structural analysis, including liquid chromatography mass spectrometry (LC-MS) and transmission electron microscopy (TEM) as analytical characterization tools for use during process development of adenovirus-based vaccines. These analytical tools provide a greater degree of complementary product understanding, with TEM providing evidence of viral particle morphology and LC-MS allowing measurement of the viral proteome.

Chimpanzee Adenovirus (ChAdOx1) and Human Adenovirus Type 5 (Ad5), two vectors typically used in commercial manufacturing, were characterized in this study. Both viral vectors were isolated *via* caesium chloride density gradient ultracentrifugation and additionally for Ad5, anion exchange membrane chromatography, to evaluate the heterogeneity of the purified Adenoviruses. One of the issues with manufacturing of adenoviruses is the presence of product related impurities such as empty and immature (non-infectious particles). [11] Whilst the assays currently employed characterize their presence and ratio, they do not provide root cause information that could be used to elucidate cause(s) of these impurities, so that they may be rationally designed out of the manufacturing process.

There is currently ongoing research in the adeno-associated virus (AAV) field to increase understanding on which features of the AAV correlate to potency [12]. Recently experiments by high-resolution native mass spectrometry investigated the composition of several AAV serotypes and highly heterogenous populations of capsids with variable composition were found [13].

Product related impurities in Adenoviruses can arise from the different stages of the virus maturation cycle of the virus particle, which undergoes a series of structural changes (Figure 1). These structural changes are governed by key adenovirus proteins which are involved in capsid assembly, DNA packaging and maturation of the particle. The key adenovirus proteins and their functions are listed in Table 1 and as part of the maturation process, many of these adenovirus proteins undergo proteolytic cleavage [11] as indicated. In addition, product related impurities may arise through mis-packaging and proteolytic cleavage; empty viral particles may have been harvested before maturation or may have been the result of errors in the packaging process that arrested maturation. The temporal sequence of events for maturation has many unanswered questions. [11]

Adenovirus shell proteins IIIa, VI and VIII, and core proteins VII, μ and TP are synthesized as precursors, and processed by the adenovirus protease (AVP) during assembly [11]. A quantitative proteomics study gave an indication of the AVP copy number, with only seven AVP molecules per viral particle [14]. Approximately, 2000 cleavages have to happen in each virion, leading to ~40 to ~300 cleavages per AVP copy [11]. These cleavages must take place internally in the highly crowded environment of the viral core as they interact with the viral DNA. The packaging scaffold L1 52/55k protein had been predicted to undergo cleavage by AVP [15]. Immature particles contain ~50 copies of full length L1 52/55k, and this protein is absent from mature virions [11 15].

Therefore, these viral proteins are potentially indicative markers of adenovirus maturation and may be observed via LC-MS to monitor the structure and ratios of various Ad5 particles. As some of the surface viral proteins have low copy numbers, they may be difficult to identify by LC-MS [11]. Additionally, the structural changes the particles undergo may cause morphological changes that can be observed using TEM[16]. Ultimately, these two methods could potentially be used to detect Ad5 product impurities and

heterogeneity for process development, and the identified marker proteins could potentially be the basis for ELISA-based assays for use in quality control, GMP settings.

Journal Pre-proof

Journal Pre-proof

Material and Methods

Cell lines and virus lab production

The human embryonic kidney cell line (HEK293) was obtained from the American Type Culture Collection (ATCC, USA) and grown to 80% confluency and passaged in Dulbecco's modified Eagle's medium (DMEM, with GlutaMAX, 4.5g/L glucose and pyruvate) containing 10% fetal bovine serum (FBS; Hyclone, USA), 100 U/mL of Penicillin G, and 100 µg/ml of Streptomycin (Thermo Fisher Scientific). Cells were cultured in a 5% CO_2 atmosphere at 37°C. Human adenovirus serotype 5 (Ad5) was prepared by seeding HEK293 cells at 2.1 x10^6 cells/mL in T-175 flasks and incubating for 24 hrs, after which the cells were infected with Ad5 virus stock (5.2×10^9 PFU/mL) at a multiplicity of infection (MOI) of 10. The cells were harvested 48 hrs post-infection when approximately 80% cytopathic effect was observed.

ChAdOx1 Vector CsCl and AEX purification

ChAdOx1-GFP and ChAdOx1 nCoV-19 vectors were prepared using the lab-scale production method described previously [17] and were purified by CsCl density-gradient ultracentrifugation by the Jenner Institute Viral Vector Core facility. Large-scale ChAdOx1 nCoV-19 vector was prepared using an AEX process based on methods described previously [9].

Ad5 CsCl purification

Infected cells (150 mL) were spun at 300 x g for 20 min, the supernatant was removed, and the cell pellet was resuspended in 13 mL of lysis buffer (50 mM Tris (pH 9.0), 0.1% Triton X-100 and 2 mM $MgCl_2$, with 25 µL nuclease added just before use) and transferred to a 50 mL centrifuge tube. The suspension was incubated at RT for 30 mins and 6 mL 5M NaCl was added. The sample was spun at 1900 x g for 5 mins and the supernatant recovered. The clarified supernatant (~18 mL) was transferred to the top of CsCl step gradient (1.25 g/cm and 1.35 g/cm CsCl solution) in 38.5 ml Beckman ultra-clear ultracentrifuge tubes. The ultracentrifugation tubes were filled to the top with HEPES buffer and

centrifuged in a Beckman SW20Ti rotor at 100,000 x g in a Beckman ultracentrifuge at 4°C for 2 hrs. The virus band containing the enriched complete particles was extracted and mixed with 1.35 g/mL CsCl solution and subjected to another round of ultracentrifugation at 100,000 x g for 18 hrs. The virus band was collected in 5 mL volume and dialyzed in Float-A-Lyzer® 100 K dialysis device (Repligen) against 1L of 50 mM Tris pH 8.0 buffer for 2 hrs. The virus samples were aliquoted and stored at -80°C.

Ad5 AEX purification

The AEX purification was performed according to the procedures described previously [17]. Briefly, the infected cells were lysed by incubating with lysis buffer (10% v/v Polysorbate 20, 50% w/v Sucrose, 20 mM $MgCl_2$, 500 mM Tris pH 8.0) with benzonase (50 unit/mL) for 2 hrs at 37°C with shaking at 110 rpm. The lysate was then clarified using a 23cm^2 HC pro depth filter (Millipore) followed by TFF step to concentrate and buffer exchange the lysate for the capture step. Using an Akta Pure (GE) a 0.18 mL bed volume Mustang Q-XT Acrodisc column (Pall) was loaded with diafiltered material at 5mL/min. Subsequently, column was washed with 5 column volumes of loading buffer (100 mM NaCl, 1 mM MgCl2, 0.1% v/v Polysorbate 20, 5% w/v Sucrose, 50 mM Bis-Tris, pH 6.5) and bound virus was eluted by a linear gradient of NaCl in elution buffer (1 M NaCl, 1 mM $MgCl_2$, 0.1% v/v Polysorbate 20, 5% w/v Sucrose, 50 mM Tris-HCl, pH 8.0). The purified virus was buffer exchanged against 1L of 50 mM Tris pH 8.0 buffer for 2 hrs, aliquoted and stored at -80°C.

Infectivity Assay

To measure the titer of infective Ad5 particles, an anti-Hexon immunostaining assay kit (Cell Biolabs Inc) was used [18]. A total of 2.5×10^5 HEK293 cells were cultured per well in 24-well plates 24 hrs before the infection. Serially diluted Ad5 virus was added to each well and cells were incubated for 48 hrs at 37°C in 5% CO_2. Briefly, cells were fixed by adding 100% cold methanol to each well and incubated at -20°C for 10 min. The cells were washed with three times and then blocked with 1% bovine

Journal Pre-proof

serum albumin (BSA) in phosphate buffered saline (PBS). The anti-Hexon polyclonal antibody followed by secondary anti mouse horseradish peroxidase (HRP) conjugated antibody (Cell Biolabs Inc.) were added sequentially to each well according to the manufacturing instructions. Staining was developed by addition of 3,3′ diaminobenzidine (DAB) substrate, and positive brown/black stained cells were counted by light microscopy and infectious titers (IFU/mL) were calculated for each well using the instruction on the kit.

Real-time quantitative PCR

All primers, probes and controls were from Adeno-X™ qPCR Titration Kit (Takara, Japan). Viral DNA was extracted from purified Ad5 using the NucleoSpin Virus kit (MN, Germany) according to the manufacturer's instructions and eluted in 30 µL of DNase and RNase-free water and stored at -20°C until use. Serial dilutions of the viral DNA sample were used as a template for qPCR to determine the threshold cycle (Ct) for each dilution. Real-time PCR assays were carried out in triplicate in a 25 µL final volume that included 2 µL of sample dilution, 12 µL of TB Green Advantage qPCR Premix (2X), 0.5 µL 50 × ROX Reference Dye, 0.5 µL of each primer (10 µM), and 9 µL of nuclease-free water on a CFX Connect (Biorad, USA) Real-Time PCR detection system under the following conditions: Denaturation at 95°C for 30 sec, then qPCR for 40 cycles at 95°C for 5 sec and 60°C for 30 sec and finally for dissociation curve, 15 sec at 95°C, 30 sec at 60°C and 15 sec at 95°C. The DNA copy number was then determined from a standard curve generated from a standard control with known genome copy number.

Reversed-Phase HPLC Analysis

ChAdOx1-GFP or Ad5 fractions were injected neat or were concentrated 10X using 100 kDa MWCO centrifugal filters (Millipore Sigma) prior to reversed-phase analysis. Adenovirus samples were injected into a 1220 LC system (Agilent Technologies) containing a Hypersil GOLD^{TM} C4 column (4.6 x 250 mm, 5 µm, ThermoFisher Scientific). The LC gradient consisted of 20-65% B (A: 0.1% trifluoroacetic acid in water, B: 0.1% trifluoroacetic acid in acetonitrile) over 90 min at a flow rate of 0.2

mL/min. Elution of each protein was monitored using the absorbance signal at 214 nm (UV214). For identification, peaks were collected manually and dried overnight at 30°C using a vacufuge (Eppendorf). The following day, a digestion solution (50 mM ammonium bicarbonate pH 7.7, 10 mM DTT, 10% acetonitrile) was added and the samples were incubated overnight at 37°C in the presence of 5 µg of trypsin or chymotrypsin. The samples were then subjected to LC-MS peptide mapping as described below.

LC-MS Peptide Mapping

ChAdOx1-GFP, ChAdOx1 nCoV-19, or Ad5 fractions were buffer exchanged into 50 mM Tris, 1 mM EDTA pH 8.0 using 100 kDa MWCO centrifugal filters (Millipore Sigma). The samples were then reduced using 10 mM DTT (5 min at 90°C), alkylated using 20 mM IAM (30 min at ambient temperature), and digested using 10 µg trypsin or chymotrypsin (overnight at 37°C). LC-MS peptide mapping was performed using a 1290 LC system (Agilent Technologies) connected in-line to a 6545XT quadrupole time-of-flight mass spectrometer (Agilent Technologies). Peptides were desalted and separated using a CSH C18 column (2.1 x 150 mm, 1.7 µm, Waters Corporation) held at 60°C. The LC gradient consisted of 0-40% B (A: water + 0.1% formic acid, B: acetonitrile + 0.1% formic acid) over 60 min at a flow rate of 0.2 mL/min. The electrospray ionization parameters consisted of: 275°C gas temperature, 4,000V Vcap, and 175V fragmentor. Mass spectra were collected from 275-1700 m/z at 1 spectra/sec. The threshold for MS/MS analysis was 10,000 counts and the two most abundant ions were selected for CID fragmentation per cycle.

MS Data Processing

Mass spectra were processed using MassHunter Bioconfirm v10.0 software (Agilent Technologies). The Ad5 (UniProt ID UP000004992) or ChAdOx (UniProt ID UP000110857) proteomes were used for the database search. Variable modifications included: Cys alkylation, Met oxidation, and Asn deamidation. The ion abundance ratio of confirmed peptides was then used to compare the relative

Journal Pre-proof

protein abundance between CsCl fractions. The number of confirmed peptides compared between CsCl fractions ranged from 5 (L1 52/55k) to 140 (Protein II) for the ChAdOx proteins.

Following data processing using MassHunter, the presence of host cell proteins in each viral sample was investigated using Proteome Discoverer v1.4 software (ThermoFisher Scientific) and the human proteome (UniProt ID UP000005640). The criteria used to confirm the presence of an HCP was ≥2 unique peptides per identified protein.

LC-MS Peptide Data Analysis

The relative abundances of various peptides within the virus proteome were determined using a method adapted from Silva *et al*. who demonstrated that, with an internal standard, the relative abundance and therefore quantity of proteins in a protein mix can be determined by comparison of the abundance of their constituent peptides identified from peptide mapping studies. [19] We adapted the procedure without the use of an internal standard to look at the relative abundance of peptides between two Adenovirus samples, and thus identified trends in the differences observed. We compared the ratios of all common peptides observed between the two Adenovirus samples being compared, rather than the top 3 most abundant as previously described [19], and then used box-whisker plots so that all the data were evaluated. For each of the ChAdOx1-GFP samples analyzed, the peptides identified from mass spectrometry peptide mapping (following trypsin and chymotrypsin digestion of the virus sample) were compared pair wise with the 2nd HDF and the relative proportion of the peptide abundance was determined for each viral protein identified. For ease of comparison, the relative abundance ratios determined for each sample were normalized against a viral protein that is known to not be modified during adenovirus assembly and maturation and that had greater than 3 common peptides identified. For relative comparisons of the different ChAdOx1-GFP CsCl fractions, the ratios were normalized against the Protein IX median ratio to be consistent with the HPLC peak area analysis in Figure 4a. For relative comparisons of the ChAdOx1 nCoV-19 samples from a large-scale AEX preparation and two lab-scale CsCl preparations, the ratios

Journal Pre-proof

were normalized against the Protein II median ratio, as too few common protein IX peptides were identified.

Transmission Electron microscopy

Copper 200 mesh grids coated with continuous carbon (Agar Scientific Ltd. Essex, UK) were glow discharged for 60 sec just before use. 5 μL of sample were incubated on the grid for 1 min, blotted and then incubated with freshly filtered 5 μL 2% uranyl acetate (UA) (Merck Life Science UK Ltd. Dorset, UK) for 1 min, blotted, dried and then imaged.

Micrographs were collected on a Tecnai T12 G2 Twin microscope equipped with a LaB6 electron source and TVIPS F216 CCD camera. All micrographs were collected with a defocus value between 3 μm and 10 μm depending on the magnification.

Virus morphology analysis

Two datasets were collected for each purified Ad5 and ChAdOx1-GFP sample fraction. The cryo EM automated particle picking software SHPIRE-crYOLO was used to train two separate models based on the main morphological classes of virus particle observed in the micrographs[20]. The micrographs from the first dataset were used exclusively for training models by manually picking full or empty capsids. A particle was deemed "complete" if the contrast across the particle diameter was uniform, suggesting no stain infiltration. "incomplete" was characterized as having darker contrast in the capsid core and a lightly contrasting periphery (Supplemental Figure 1).

Models were built separately for Ad5-full, Ad5-empty, ChAdOx1-GFP-full and ChAdOx1-GFP-empty and then used for automated picking of the second dataset for each purification condition in crYOLO. The box manager GUI within crYOLO was used to inspect the picking quality manually.

Journal Pre-proof

Results

Analysis of Ad5 of in-process samples by TEM and LC-MS

To examine the application of transmission electron microscopy (TEM) as an adenovirus product monitoring analytical tool to measure viral particle size and morphology as a quality attribute, morphological differences between Human Adenovirus serotype 5 (Ad5) particles purified using either of two purification processes, i.e., CsCl ultra-centrifugation vs. tangential flow filtration (TFF) followed by anion exchange chromatography (AEX), were assessed (Figure 2A). Representative TEM images of Ad5 produced from the two processes (Figure 2B) show that Ad5 particles with different morphological characteristics were observed. Some particles appear well ordered with consistent contrast across the capsid highlighting the triangular faces of their icosahedral structure (complete – full/immature/mature/infectious) whilst others appear less ordered, more faintly contrasting and have a less defined core (incomplete - empty). The abundance of incomplete particles appeared to be greater in the TFF-AEX purified samples compared to CsCl ultra-centrifugation. Digital analysis (see Methods) of TEM images confirms that the proportion of particles identified as being complete was higher in the samples prepared by CsCl separation (95%) when compared to samples prepared using TFF-AEX (76%). The proportion of complete viral particles correlated with the infectivity ratio, where a greater proportion of particles identified as being complete gives an improved (lower) infectivity ratio (Table 2).

To determine whether the morphological differences observed above could be monitored by the viral protein profile of the Ad5 samples from the two processes, LC-MS peptide mapping was employed (Figure 2C). The proteins identified in the individual LC peaks correlate with other reports that have characterized the Ad5 proteome using LC-MS [21] [22]. Comparisons of the Ad5 samples taken from the different purification methods did not demonstrate a clear difference in the viral protein profile observed given the method's estimated limit of quantification for smaller peaks. Nonetheless, an increased abundance of the Protein VIII(3) fragment (68 min), a known cleavage product of Protein VIII, in the CsCl purified material was visually observed. This result suggests a potential trend that more cleavage events occurred in this sample and therefore the proportion of mature particles present in this sample was

Journal Pre-proof

higher (i.e., above the limit of detection, LOD); however, such observations could not be quantitated (i.e., below the limit of quantitation, LOQ).

Analysis of ChAdOx1-GFP in-process samples by TEM and LC-MS

The same analytical characterization tools described above to evaluate in-process samples of Ad5 particles were then utilized to characterize in-process samples of Chimpanzee Adenovirus Oxford serotype Y25 (ChAdOx1-GFP). As part of this work, further development of the LC-MS peptide mapping method was carried out to improve the ability of the method to quantitate visually observable differences in smaller peaks observed in the chromatograms. Other groups that have examined various analytical tools for adenovirus particles have demonstrated the benefit of separating the empty and full particles to improve sensitivity, [7] [22] and therefore in-process samples from the different stages of CsCl ultracentrifugation purification were generated by removing the low (LDF)- and high-density fractions (HDF) from both stages of the ultracentrifugation (Figure 3A). This purification scheme resulted in generation of 4 different in-process samples of ChAdOx1-GFP: low-density fraction from first spin (1st LDF), low-density fraction from second spin (2nd LDF), high-density fraction from first spin (1st HDF) and high-density fraction from second spin (2nd HDF).

For TEM analysis, similar to result described above with the Ad5 samples, there were observable qualitative differences in the ChAdOx1-GFP particle structures in the TEM images (Figure 3B). Although CsCl ultracentrifugation could in theory completely separate 'empty' and 'full' virus particles, i.e., those that have either not been packaged with DNA (empty, LDF) and those that contain DNA (full, HDF) based on the difference in expected density, in practice the separation was not complete and only resulted in enrichment of the two species. For example, while the ChAdOx1-GFP samples in general did follow this logic (i.e., HDF contained particles with a more ordered and complete structures), empty and full particles were found in all fractions (Figure 3B). In addition, when the particles are assigned to being either incomplete or complete, a clear separation in the proportion of complete particles was observed in the different fractions (Table 3) with the LDF having 62% (1st spin) and 45% (2nd spin) and the HDF

Journal Pre-proof

having 93% (1st Spin) and 99% (2nd spin). Moreover, the increased proportion of complete particles observed in the 2nd spin HDF compared with the 1st spin HDF sample indicates the importance of the additional spin towards improving the quality of the final virus preparation. When the proportion of complete particles of ChAdOx1-GFP was compared with the measured infectivity of the different fractions there was a broad correlation, with a higher number of complete particles indicating an improved (lower) infectivity ratio (Table 3). The LDF from the 2nd spin sample, however, deviated from this correlation, which was potentially due to the low particle number in the sample and inaccuracies in the methods used to determine the infectivity ratio.

Applying LC-MS peptide mapping methodologies it was possible to characterize the profile of the viral proteins present in each of the ChAdOx1-GFP process samples and again these assignments agree with previous reports [7]. Comparison of the chromatograms from the 4 different CsCl separated fractions showed overall similar profiles (Figure 3C); however, if a visual comparison is made between the chromatograms of the two LDF and the two HDF samples, a pattern emerged where some of the smaller peaks that are present in the LDF were not visible in the HDF chromatograms. It is known that during the Adenovirus maturation process cleavage events occur such that certain viral proteins may be present in the immature particle, and not in the mature particle [15]. Through further analysis of the peak area for each viral protein determined from the chromatogram, it was possible to make a comparison of the relative abundance of each protein in each of the fractions (Figure 4A). This comparison highlights that some peaks (and associated viral proteins) are distinctly present in LDF (empty particle enriched) and are either reduced (e.g., a HCP, Histone H4 and L1 52/55k) or in some cases not present at all (e.g., the peak containing a mixture of Protein II, Protein V, Protein VI(1), and Protein VII(3)) in the HDF (full particle enriched). If the relative abundance of key peaks from the LC-MS peptide mapping data are displayed and compared in the form of a radar plot (Figure 4B), the difference between the LDFs (green and red) and HDFs (blue and black) fractions is more clearly observable.

It is worth noting that since some of these smaller peaks in the chromatograms are above the estimated limit of detection but below the estimated limit of quantitation (indicated in grey in Figure 4A

Journal Pre-proof

and 4B), and therefore the trends described above in the radar charts are qualitative in nature. When these proteins are not considered, the only peak in the chromatogram that displays differences between the LDF and HDF samples is assigned to L1 52/55k. This is a viral protein involved in the packaging and encapsulation of DNA into the capsid [11] and is known to be cleaved during the maturation process with a loss of copy number when comparing immature and mature particles. [11] This peak in the LC-MS peptide mapping chromatogram could therefore be a marker for the proportion of immature/mature particles in a given sample. This is borne out here as we would expect more immature particles, and therefore L1 52/55k, to be present in the LDFs (empty particle enriched). These data indicate that monitoring the relative abundance of L1 52/55k in the protein profile of a sample could be used to determine the abundance of empty vs packaged/mature and be a measure of the degree of maturation (Table 3).

Although information about the proportion of empty vs full ChAdOx1 particles is important, a more interesting quality marker to gain information about manufacturing processes would determine more subtle differences between samples containing full ChAdOx1 particles. When the HDF taken from the 1st CsCl spin is compared with the HDF taken from the 2nd CsCl spin (which were expected to have a more comparable profile than comparing LDFs to HDFs as described above) the relative abundance of the L1 52/55k peak was similar in the chromatogram data. The data were therefore further analyzed using a technique adapted from the literature for quantification of proteins based on the relative abundance of peptides determined from the LC-MS data [19]. Here, because the samples had not been spiked with a protein of known concentration (i.e., internal standard), absolute quantification was not determined; however, we compared samples in a pairwise manner and evaluated the relative abundance of proteins based on the abundance of their constituent peptides observed in the LC-MS analysis (see Methods).

As shown in Figure 4C, a box-whisker plot was generated that shows the ratios observed for the constituent peptides of the adenovirus proteins when performing a pairwise comparison between 1st LDF, 2nd LDF, or 1st HDF against 2nd HDF (i.e., the fraction that most closely represents the final adenovirus product). In this analysis, viral proteins that have similar abundance between two samples would have a ratio of 1, while a higher or lower ratio would indicate a concentration difference. Analyzing the data

using this method, we confirmed the change in relative abundance previously observed in L1 52/55k when comparing LDF and HDF samples, where the ratio of L1 52/55k peptides present was greater than five times in both LDF samples. Interestingly, when comparing the 1st HDF with 2nd HDF sample, a higher ratio of L1 52/55k was also observed (ratio of ~2) compared to the other Adenovirus proteins present (ratio of ~1), indicating that the 1st HDF had more L1 52/55k and therefore had a greater proportion of immature particles. Note, it was not possible to perform this analysis on the Ad5 samples as the number of common L1 52/55k peptides observed in the those in-process samples were not sufficient.

A comparison of the TEM, LC-MS peptide mapping and typical virus particle characterization data collected with in-process samples (i.e., total viral particle concentration and viral infectivity concentration) is shown in Table 3. An apparent correlation between the proportion of complete viral particles, the relative abundance of L1 52/55k, and the infectivity ratio is observed. For example, a higher number of complete viral particles (measured using TEM) was associated with a lower abundance of L1 52/55k (measured by LC-MS peptide mapping) and an improved (lower) infectivity ratio. These results suggest that both the TEM and LC-MS peptide mapping methods could potentially be used as additional quality indicators for adenovirus particles as part of processing monitoring.

To further examine the utility of the LC-MS peptide mapping method to better characterize vector quality attributes, three preparations of a second ChAdOx1 vector (ChAdOx1 nCoV-19), each with a different P:I ratio, were compared in a pairwise fashion (Figure 5). Two lab-scale viral samples were purified using CsCl ultracentrifugation (Lab-scale 1 (P:I ratio 68) or Lab-scale 2 (P:I ratio 31)), while a large-scale sample was purified using AEX chromatography (Large-scale (P:I ratio 97)). Following the LC-MS analysis and data processing of these samples, too few (i.e., < 3) common Protein IX peptides were identified to apply the same peptide abundance normalization methodology as described above. Therefore, peptide abundance was normalized to Protein II, another viral protein that is not known to be modified during adenovirus assembly and maturation. The relative abundance of the L1 52/55k peptides were 10- and 12- folder higher in the large-scale AEX purified sample (highest P:I ratio) compared to two

Journal Pre-proof

lab-scale CsCl purified samples. A comparison of Lab-scale 1 and Lab-scale 2 samples did not indicate a notable change in the relative abundance of L1 52/55k.

Discussion

The application of using adenoviruses as vectors in the biopharmaceutical sphere is becoming more widespread [23] and as such more focus has been placed on optimizing the manufacturing process. A key part of this is the development of analytical tools in parallel to monitoring both process and product contaminants to ensure that the end-product is safe. To date the product-related analytical tools that have been applied have mainly focused on traditional techniques that determine the virus particle concentration and infectivity ratio[7], although a comprehensive study of adeno-associated viral (AAV) vector manufacturing, a similar class of product, has recently demonstrated that more detailed analysis can demonstrate differences in manufacturing, allowing process decisions that lead to a more efficacious product.[12] To improve Adenovirus vaccine manufacturing, modern instrumentation and methodologies currently in use for relatively less complex biopharmaceuticals (e.g., glycan profiling of mAbs, AAV) should be evaluated for their application towards the develop of these important viral vectors. In this paper two techniques that have previously been used to study Adenovirus particles but have not necessarily been implemented to monitor the quality attributes of samples were investigated and the results demonstrate a proof of principle that both transmission electron microscopy (TEM) and liquid chromatography mass spectrometry (LC-MS) have the potential to be used for process monitoring.

Transmission Electron Microscopy (TEM) as an in-process analytical tool for Adenovirus

A key product-related contaminant in Adenovirus manufacturing is the presence of empty (incomplete) particles, i.e., particles that have a complete capsid but have not yet been packaged with DNA. They can be separated using CsCl ultracentrifugation and it has been demonstrated that TEM can be used to distinguish between empty and full (packaged) particles as stain enters the empty particles but cannot enter the full particles [22 24]. Previous reports of the use of TEM to characterize Adenovirus have

either been from a structure/function point of view[15 25] or to verify that samples are either empty or full[22] and whilst some advances have been made in using EM to characterize other therapeutic products such as rAAV [26] and virus-like particles[27] we believe further advances can be made for Adenovirus products. In this report, an automated algorithm to characterize the relative proportion of incomplete and complete virus particles in Human Adenovirus serotype 5 (Ad5) and Chimpanzee Adenovirus Oxford serotype Y25 (ChAdOx1) adenovirus samples was described and shown to be effective at distinguishing and counting the abundance of the particles. In the Ad5 samples that were purified using either CsCl ultracentrifugation or AEX separation, a greater proportion of complete particles was measured in the CsCl prepared samples, which was consistent with our observations that better separation of empty and full particles is achieved when compared to AEX chromatography. In the ChAdOx1 samples that were taken from different stages of the CsCl ultracentrifugation process, the proportion of incomplete and complete was generally consistent with the logic that the low-density fraction (LDF) contained more incomplete particles while the high-density fraction (HDF) contained more complete particles. In addition, the second CsCl purification step further improves the ratio of complete particles. This measure of the proportion of incomplete particles is an important quality metric as it will impact the proportion of active particles in the final product and indirectly the required dose. This relative proportion of incomplete/complete particles also gave an indication of the infectivity of the sample.

Liquid Chromatography - Mass Spectrometry (LC-MS) peptide mapping as an in-process analytical tool for Adenovirus

LC-MS peptide mapping is a commonly used analytical tool for the characterization of therapeutic proteins and their critical quality attributes but has not to our knowledge been applied to the characterization of Adenovirus quality/infectivity to aide process development. Utilizing two different Adenovirus vectors, the LC-MS-based peptide mapping techniques identified the constituent proteins of the Adenovirus particles, and their reversed-phase LC (RP-LC) elution profiles were overall similar to that of previous reports [28 21 29 7 22]. Analysis of the relative peak area for different proteins from Ad5

Journal Pre-proof

samples purified by either CsCl centrifugation or TFF-AEX chromatography showed that no substantial differences were observed. A comparison of the ChAdOx1 fractions taken from different stages of CsCl ultracentrifugation, however, demonstrated that a notable difference in the peak area for L1 52/55K could be observed, with viral particles taken from the LDF (empty particle enriched) showing a greater abundance of this protein than in the HDF (full particle enriched). This change in peak area is also observed in the RP-HPLC chromatograms from other studies that have investigated LDF and HDF [7 22].

The relative abundance of L1 52/55k peptides between the CsCl fractions not only supported the observations made by RP-HPLC when comparing the LDF and HDF, but also was able to detect a difference in these same L1 52/55k peptides in the HDF from the 1st and 2nd CsCl ultracentrifugation samples. Taken together, these results indicate that relative peptide abundance analysis via LC-MS peptide mapping data (a more sensitive technique than comparison of integrated HPLC peak area) facilitates identification of relative differences between samples and therefore is potentially a useful approach to detect differences in Adenovirus product quality within process samples. When the LC-MS technique was applied to a second ChAdOx1 vector (ChAdOx1 nCoV-19) that was purified using different procedures, a clear difference in L1 52/55k was observed, indicating how a change in purification method may have an impact on the quality of a sample (it is noted that the large-scale purification material was taken from an early process development run that would not have been fully optimized). The differences in ratio values of L1 52/55k between the ChAdOx1-GFP CsCl fractions (~5 fold) or the ChAdOx1 nCoV-19 AEX vs CsCl purified material (~10-12 fold) is potentially an informative metric for vector product quality and correlated with known P:I ratios. At the same time, this technique was unable to differentiate the relative abundance of the L1 52/55k protein between two ChAdOx1 nCoV-19 lab-scale CsCl purified samples with different P:I ratios (i.e., 68 vs. 31).

Based on these results, additional method development with LC-MS peptide mapping is needed as part of future work to better characterize in-process materials including (1) increasing the sensitivity of the analytical technique, (2) and/or pairing results with additional assays (e.g., TEM). One complication in implementing LC-MS into a manufacturing workflow is the noted relative low abundance of L1 52/55k

Journal Pre-proof

and other virus components in HDF samples. Therefore, the LC-MS method requires further development to increase the technique's sensitivity and more precisely quantify the abundance of each component within an Adenovirus in-process sample. For example, sensitivity could be increased by loading more sample, but optimizing chromatographic components (e.g., column chemistry, column temperature, mobile phase composition) would likely be required to maintain peak resolution. The addition of an internal standard of know concentration should also be investigated to accurately quantify the abundance of each viral protein during processing and purification. Finally, the required use of two different adenovirus proteins (Protein IX and Protein II) for peptide normalization in two studies presented in this work indicate that a more consistent viral protein benchmark could be identified to increase the utility of a LC-MS as an in-process analytical tool for adenovirus manufacturing.

The monitoring of the abundance of the L1 52/55k protein as a quality indicator could be beneficial as it is not only involved in the packaging of DNA, but also its cleavage and release from the virus particle is thought to be part of the maturation process [11 30 25 15] as it is not found in fully matured particles. Perez-Berna *et al.*, have recently suggested a model whereby L1 52/55k is involved in anchoring of the DNA to the inner side of the viral capsid, proposing that's its cleavage and expulsion is linked to DNA condensation within the particle. Given its role in virus assembly, the relative abundance of L1 52/55k determined by LC-MS peptide mapping could be a good in-process marker to monitor viral particle maturation status during Adenovirus downstream processing and purification.

Journal Pre-proof

Conclusion

In this study, two higher resolution analytical techniques as potential tools for the characterization of adenovirus vector quality during process development were evaluated. First, Human Adenovirus serotype 5 (Ad5) TEM analysis demonstrated that a higher abundance of complete particles correlates with an improved (lower) infectivity ratio in samples prepared by either CsCl ultracentrifugation (95% complete particles, P:I ratio 4) or AEX chromatography (76% complete particles, P:I ratio 14). This correlation was confirmed in CsCl ultracentrifugation prepared ChAdOx1-GFP samples taken from the 1st

and 2nd LDF (62/45%, P:I ratio 113/77) and the 1st and 2nd HDF (93/99%, P:I ratio 79/56). Second, ChAdOx1-GFP LC-MS peptide mapping analysis also demonstrated a correlation between the infectivity ratio and a specific readout (the relative abundance of L1 52/55k) in vector samples including LDF (5.5/5.6, P:I ratio 113/77) and HDF (2.0/1.0, P:I ratio 79/56). The utility of the LC-MS peptide mapping method was further evaluated using a second ChAdOx1 vector (ChAdOx1 nCoV-19) purified by CsCl ultracentrifugation or AEX chromatography, and a 10 to 12 fold difference in the relative abundance of L1 52/55k was observed in the AEX sample (P:I ratio 97) compared to the CsCl samples (P:I ratios of 68 and 31). Taken together, the data presented in this work shows the proportion of incomplete vector particles determined by TEM image analysis and the abundance of L1 52/55K determined by LC-MS peptide abundance analysis correlates with the infectivity ratio measured using more standard cell-based techniques, e.g., with HDF samples showing a lower abundance of empty (incomplete) particles and the protein L1 52/55k compared with LDF. While the presented results are an encouraging initial step, both TEM and LC-MS peptide mapping techniques offer the potential to provide an even more data-rich datasets about the quality of Adenovirus vector samples and demonstrate their value as process development tools. Given the importance of Adenovirus-based vectors, gaining a greater understanding of the manufacturing process and its impact on product quality/infectivity using higher-resolution analytical tools is critical in improving manufacturing consistency and reducing costs.

Journal Pre-proof

Acknowledgements

We are grateful to Claire Powers and the Jenner Institute Viral Vector Core Facility for skilled assistance and provision of ChAdOx1-GFP and ChAdOx1 nCoV-19 samples. This work was supported, in whole or in part, by the Bill & Melinda Gates Foundation [OPP1154682]. Under the grant conditions of the Foundation, a Creative Commons Attribution 4.0 Generic License has already been assigned to the Author Accepted Manuscript version that might arise from this submission.

Data availability statement

The datasets generated and/or analyzed during the current study are available in the KU ScholarWorks repository, https://doi.org/10.17161/1808.33700. The data is also available with the corresponding author(s).

Journal Pre-proof

Table Legends

Table 1. Key adenoviral structural proteins and their functional characteristics.[30]

Table 2. TEM analysis of transmission electron microscopy images of Ad5 samples purified by CsCl ultracentrifugation or anion exchange chromatography.

Table 3. Analytical comparison of TEM; LC-MS and virus particle data for ChAdOx1 fractions taken from CsCl ultracentrifugation purification. [α]relative peak abundance determined from RP-UHPLC. [β]median relative abundance of L1 52/55k determined from peptide analysis.

Figure Legends

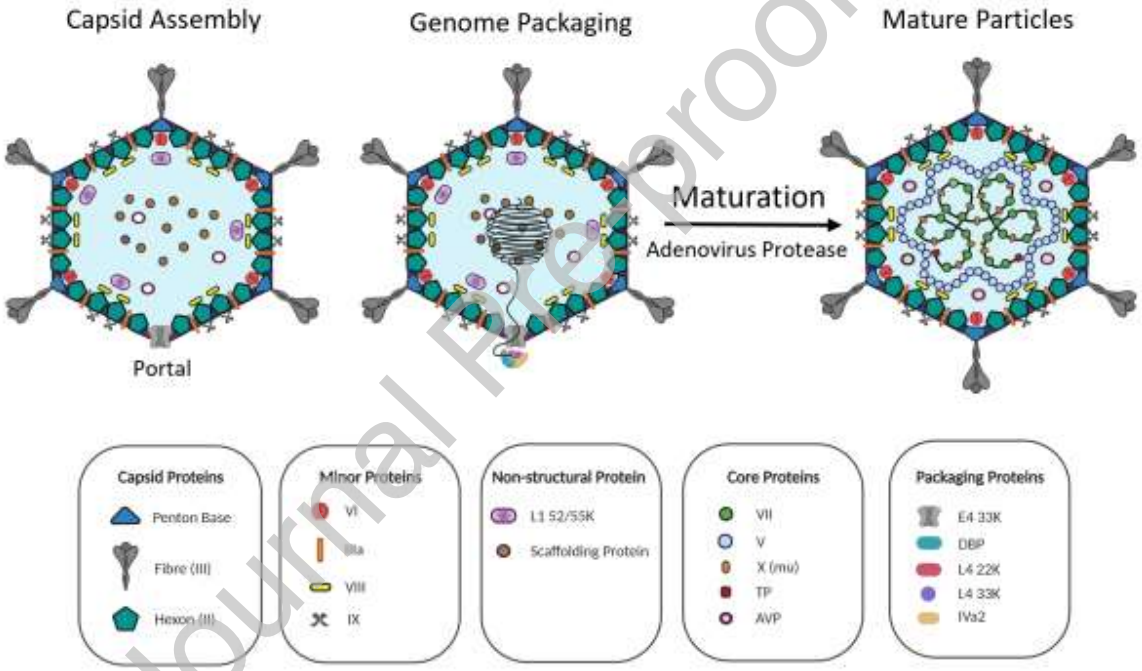

Figure 1. Schematic of the processes that are involved in the formation and maturation of adenovirus particles. Capsids are first assembled with one vertex acting as a portal. Packing proteins associate with the portal vertex and the viral DNA, transporting the DNA into the assembled capsid. Maturation to an infectious adenovirus particle occurs through cleavage of key adenovirus proteins by adenovirus protease (AVP) and condensation of the viral DNA. Images Created with BioRender.com

Journal Pre-proof

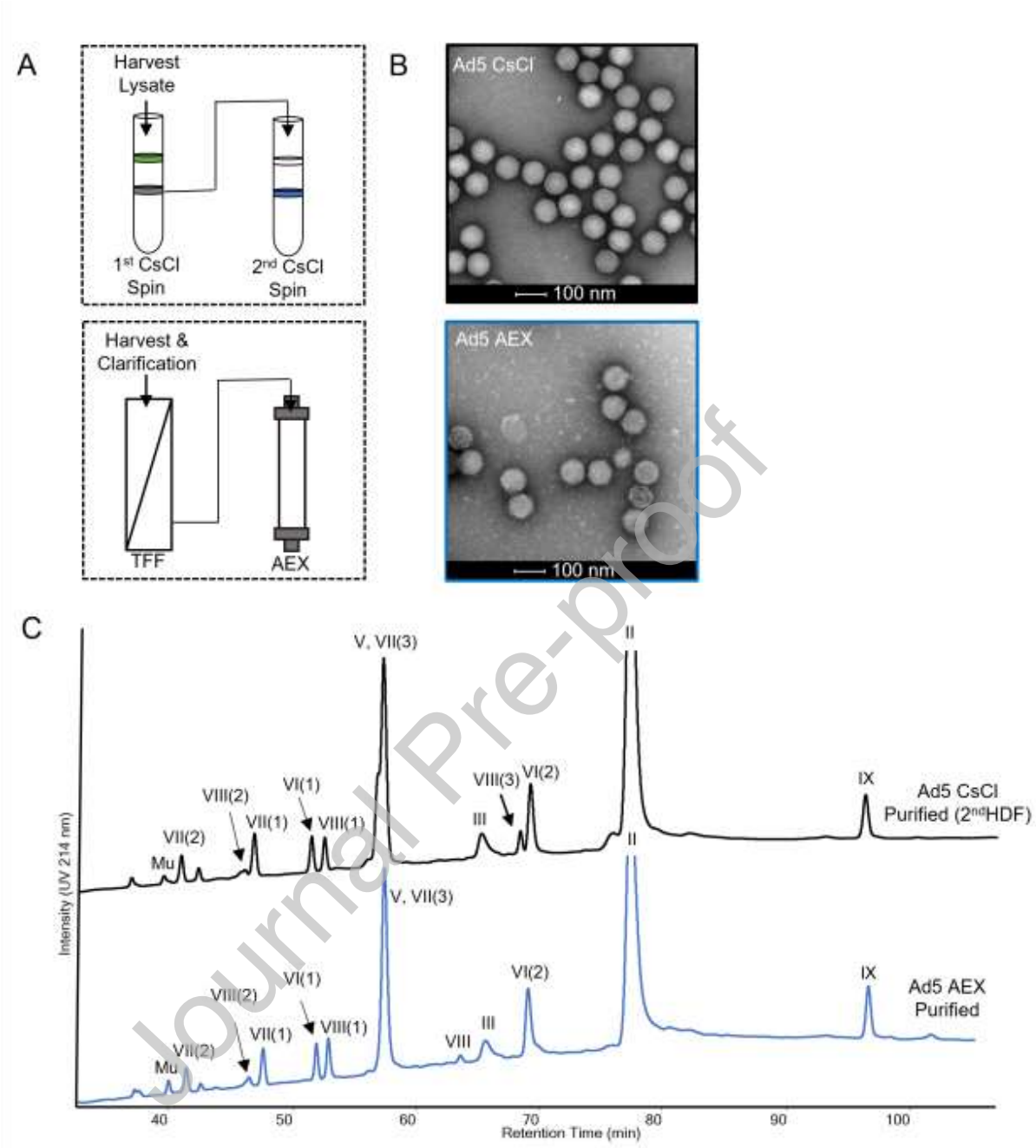

Figure 2. Characterization of appearance and composition of Ad5 samples during CsCl ultracentrifugation or TFF-AEX purification. (A) Flow diagram of purification of Ad5 fractions. (B) Representative TEM micrographs of Ad5 samples taken from high density fraction of 2nd CsCl spin and eluant from AEX with 100 nm scale bars. (C) Representative RP-UHPLC chromatograms of CsCl (black trace) or AEX (blue trace) purified Ad5. The Ad5 protein comprising each peak were identified through LC-MS peptide mapping.

Journal Pre-proof

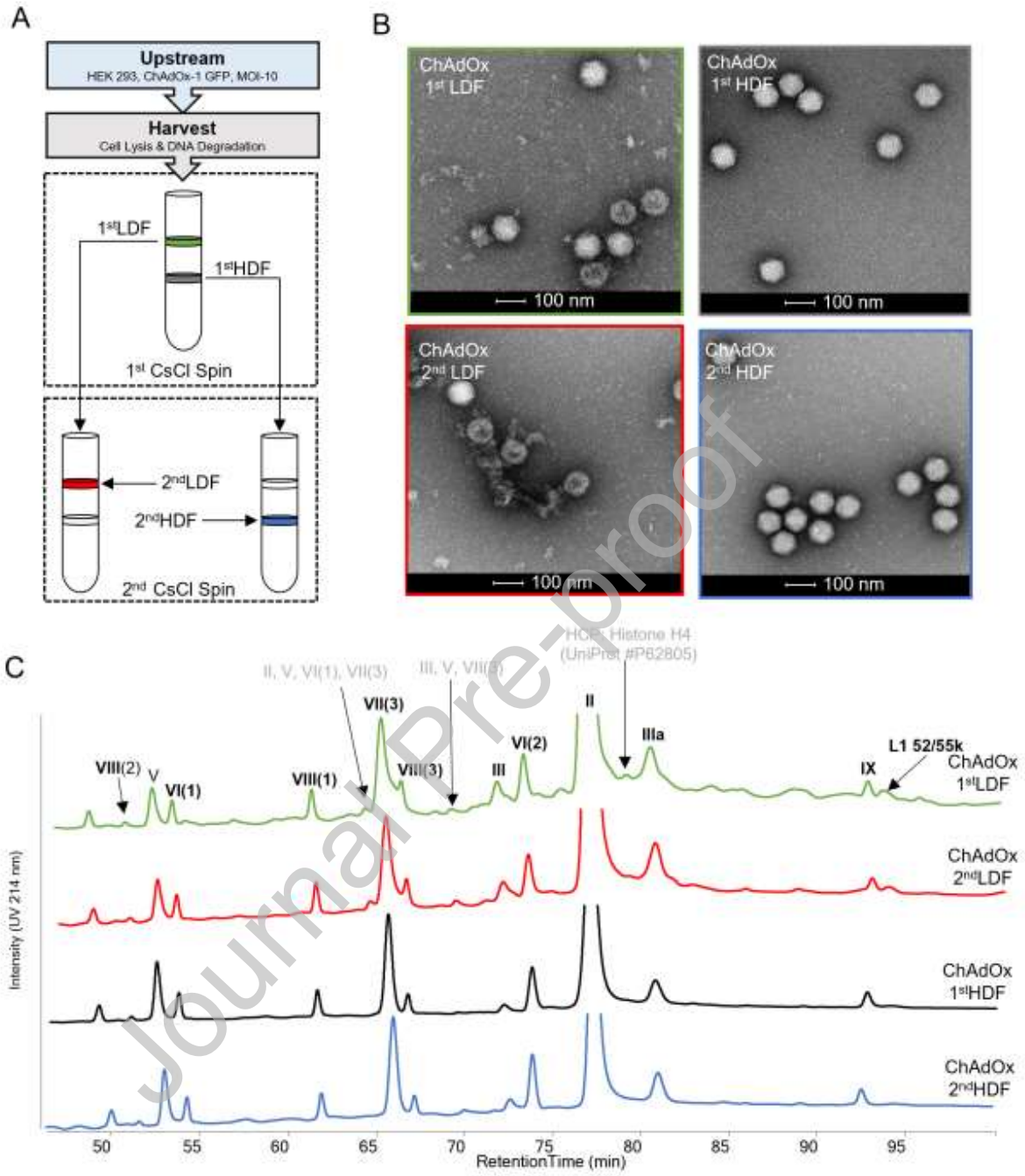

Figure 3. Characterization of appearance and composition of ChAdOx1-GFP samples during CsCl purification. (A) Flow diagram of ChAdOx1-GFP fractions. (B) Representative TEM micrographs of LDF or HDF ChAdOx1-GFP from the 1st or 2nd CsCl purification step with 100 nm scale bars. (C) Representative RP-UHPLC chromatograms of CsCl purified ChAdOx1-GFP. The first or second CsCl

low density fractions (LDF) are shown in green or red, respectively, while the first or second CsCl high density fractions (HDF) are shown in black or blue, respectively.

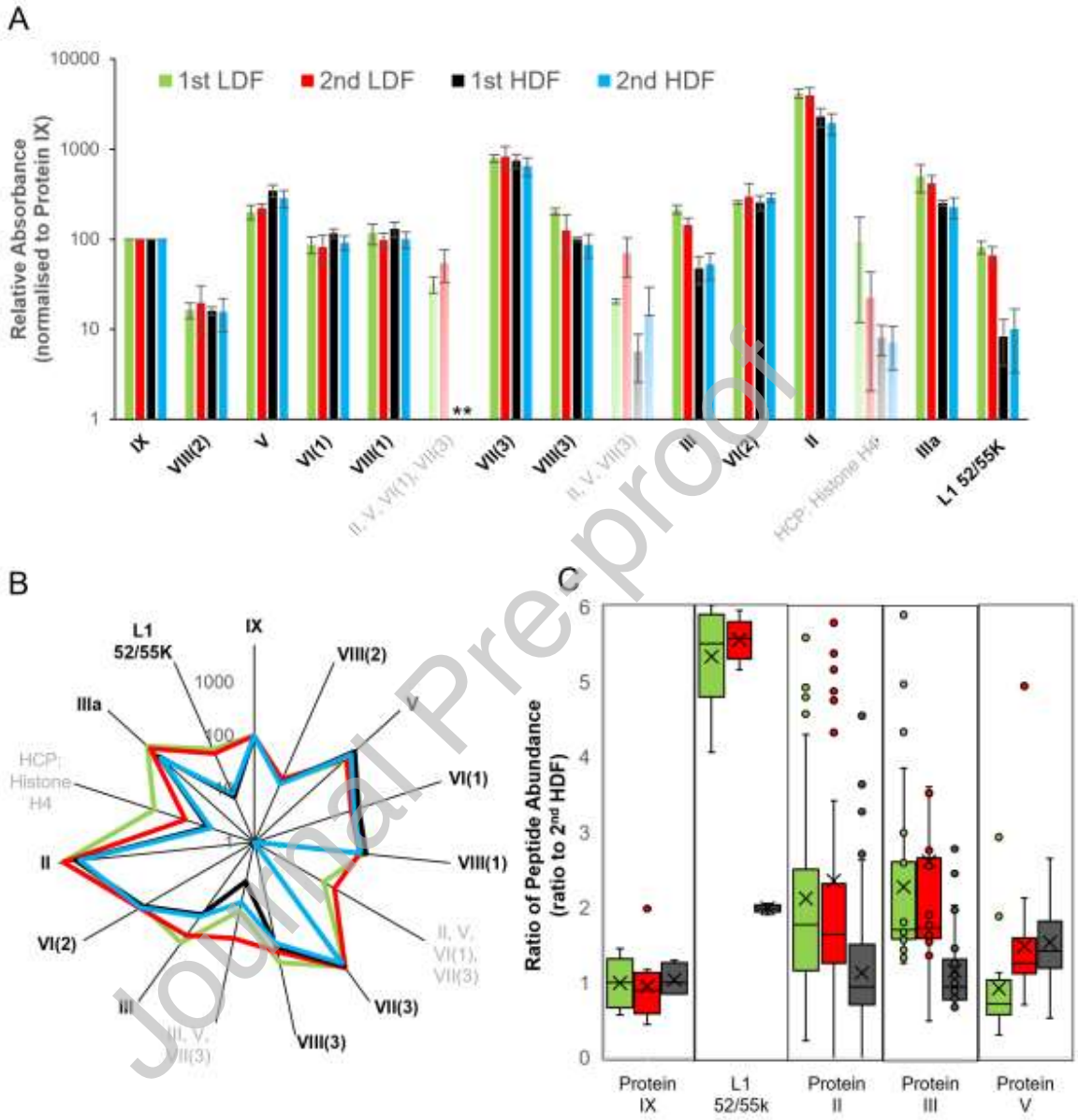

Figure 4. Comparison of relative protein quantification approaches of LC-MS peptide map datasets from ChAdOx1-GFP samples from purification process. (A) Relative RP-UHPLC peak comparison between the different ChAdOx1-GFP CsCl fractions. RP-UHPLC peak abundancies in each CsCl fraction were normalized to the Protein IX peak. Error bars represent triplicate MS measurements. The asterisks (*) denotes a peak not observed in the HDF samples. (B) A radar plot visualization of the same datasets in panel (A). Proteins indicated in grey are below the limit of quantitation. (C) Relative peptide abundance for representative viral proteins in the ChAdOx1-GFP CsCl fractions when compared pairwise to the 2nd

high density fraction. Box represents interquartile range, error bars represent range, dots represent outliers and X represents mean. Number of peptides compared is dependent on samples and protein, but n >4.

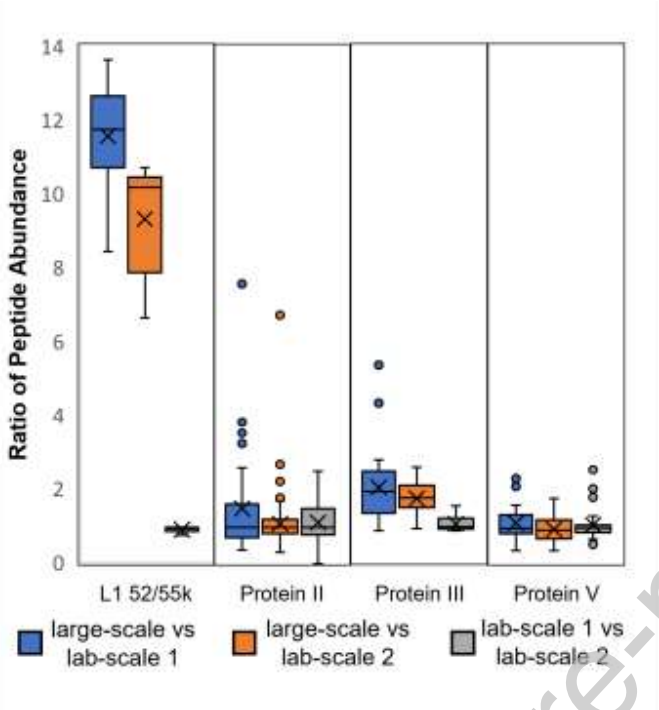

Figure 5. ChAdOx1 nCoV-19 peptide analysis. Relative peptide abundance for representative proteins in the ChAdOx1 nCoV-19 samples as measured by LC-MS peptide mapping, Samples analysed were taken from one large-scale AEX preparation and two different lab-scale CsCl preparations with different P:I ratios and results were compared pairwise for the ratio of peptide abundance for four different viral proteins. 3 different comparisons are shown: blue boxes - Large-scale AEX (P:I ratio 97) and Lab-scale CsCl 1 (P:I ratio 68); orange boxes - Large-scale AEX (P:I ratio 97) and Lab-scale CsCl 2 (P:I ratio 31); grey boxes - Lab-scale CsCl 1 (P:I ratio 68) and Lab-scale CsCl 2 (P:I ratio 31). Box represents interquartile range, error bars represent range, dots represent outliers and X represents mean. Number of peptides compared is dependent on samples and protein but always >4.

Declaration of interests

☐ The authors declare that they have no known competing financial interests or personal relationships that could have appeared to influence the work reported in this paper.

Reference

1. Barnes LF, Draper BE, Jarrold MF 2022. Analysis of recombinant adenovirus vectors by ion trap charge detection mass spectrometry: accurate molecular weight measurements beyond 150 MDa. Analytical Chemistry 94(3):1543-1551.
2. SM Wold W, Toth K 2013. Adenovirus vectors for gene therapy, vaccination and cancer gene therapy. Current gene therapy 13(6):421-433.
3. Lee CS, Bishop ES, Zhang R, Yu X, Farina EM, Yan S, Zhao C, Zeng Z, Shu Y, Wu X 2017. Adenovirus-mediated gene delivery: potential applications for gene and cell-based therapies in the new era of personalized medicine. Genes & diseases 4(2):43-63.
4. Crystal RG 2014. Adenovirus: the first effective in vivo gene delivery vector. Human gene therapy 25(1):3-11.
5. Evans RK, Nawrocki DK, Isopi LA, Williams DM, Casimiro DR, Chin S, Chen M, Zhu D-M, Shiver JW, Volkin DB 2004. Development of stable liquid formulations for adenovirus-based vaccines. Journal of pharmaceutical sciences 93(10):2458-2475.
6. Pelliccia M, Andreozzi P, Paulose J, D'Alicarnasso M, Cagno V, Donalisio M, Civra A, Broeckel RM, Haese N, Jacob Silva P 2016. Additives for vaccine storage to improve thermal stability of adenoviruses from hours to months. Nature communications 7(1):1-7.
7. Mullins EK, Powers TW, Zobel J, Clawson KM, Barnes LF, Draper BE, Zou Q, Binder JJ, Dai S, Zhang K 2021. Characterization of recombinant chimpanzee adenovirus C68 low and high-density particles: impact on determination of viral particle titer. Frontiers in Bioengineering and Biotechnology 9.
8. Jothikumar N, Cromeans TL, Hill VR, Lu X, Sobsey MD, Erdman DD 2005. Quantitative real-time PCR assays for detection of human adenoviruses and identification of serotypes 40 and 41. Applied and environmental microbiology 71(6):3131-3136.
9. Joe CC, Jiang J, Linke T, Li Y, Fedosyuk S, Gupta G, Berg A, Segireddy RR, Mainwaring D, Joshi A 2022. Manufacturing a chimpanzee adenovirus‐vectored SARS‐CoV‐2 vaccine to meet global needs. Biotechnology and bioengineering 119(1):48.
10. Lusky M 2005. Good manufacturing practice production of adenoviral vectors for clinical trials. Human gene therapy 16(3):281-291.
11. Mangel WF, San Martin C 2014. Structure, Function and Dynamics in Adenovirus Maturation. Viruses 6(11):4536-4570.
12. Rumachik NG, Malaker SA, Poweleit N, Maynard LH, Adams CM, Leib RD, Cirolia G, Thomas D, Stamnes S, Holt K 2020. Methods matter: standard production platforms for recombinant AAV produce chemically and functionally distinct vectors. Molecular Therapy-Methods & Clinical Development 18:98-118.
13. Wörner TP, Bennett A, Habka S, Snijder J, Friese O, Powers T, Agbandje-McKenna M, Heck AJ 2021. Adeno-associated virus capsid assembly is divergent and stochastic. Nature communications 12(1):1-9.
14. Benevento M, Di Palma S, Snijder J, Moyer CL, Reddy VS, Nemerow GR, Heck AJ 2014. Adenovirus composition, proteolysis, and disassembly studied by in-depth qualitative and quantitative proteomics. Journal of Biological Chemistry 289(16):11421-11430.
15. Pérez-Berná AJ, Mangel WF, McGrath WJ, Graziano V, Flint J, Martín CS 2014. Processing of the L1 52/55k Protein by the Adenovirus Protease: a New Substrate and New Insights into Virion Maturation. Journal of Virology 88(3):1513-1524.
16. Rux JJ, Burnett RM 2004. Adenovirus structure. Human gene therapy 15(12):1167-1176.
17. Fedosyuk S, Merritt T, Peralta-Alvarez MP, Morris SJ, Lam A, Laroudie N, Kangokar A, Wright D, Warimwe GM, Angell-Manning P, Ritchie AJ, Gilbert SC, Xenopoulos A, Boumlic A,

Douglas AD 2019. Simian adenovirus vector production for early-phase clinical trials: A simple method applicable to multiple serotypes and using entirely disposable product-contact components. Vaccine 37(47):6951-6961.
18. Dicks MD, Spencer AJ, Edwards NJ, Wadell G, Bojang K, Gilbert SC, Hill AV, Cottingham MG 2012. A novel chimpanzee adenovirus vector with low human seroprevalence: improved systems for vector derivation and comparative immunogenicity. PloS one 7(7):e40385.
19. Silva JC, Gorenstein MV, Li G-Z, Vissers JPC, Geromanos SJ 2006. Absolute Quantification of Proteins by LCMS: A Virtue of Parallel ms Acquisition * S. Molecular & Cellular Proteomics 5(1):144-156.
20. Wagner T, Merino F, Stabrin M, Moriya T, Antoni C, Apelbaum A, Hagel P, Sitsel O, Raisch T, Prumbaum D 2019. SPHIRE-crYOLO is a fast and accurate fully automated particle picker for cryo-EM. Communications biology 2(1):1-13.
21. Lehmberg E, Traina JA, Chakel JA, Chang R-J, Parkman M, McCaman MT, Murakami PK, Lahidji V, Nelson JW, Hancock WS 1999. Reversed-phase high-performance liquid chromatographic assay for the adenovirus type 5 proteome. Journal of Chromatography B: Biomedical Sciences and Applications 732(2):411-423.
22. Takahashi E, Cohen SL, Tsai P, Sweeney JA 2006. Quantitation of adenovirus type 5 empty capsids. Analytical biochemistry 349(2):208-217.
23. Zhao Z, Anselmo AC, Mitragotri S 2022. Viral vector‐based gene therapies in the clinic. Bioengineering & translational medicine 7(1):e10258.
24. D'Halluin J, Milleville M, Boulanger P, Martin G 1978. Temperature-sensitive mutant of adenovirus type 2 blocked in virion assembly: accumulation of light intermediate particles. Journal of Virology 26(2):344-356.
25. Condezo GN, Marabini R, Ayora S, Carazo JM, Alba R, Chillón M, San Martín C 2015. Structures of adenovirus incomplete particles clarify capsid architecture and show maturation changes of packaging protein L1 52/55k. Journal of virology 89(18):9653-9664.
26. Colomb-Delsuc M, Raim R, Fiedler C, Reuberger S, Lengler J, Nordström R, Ryner M, Folea IM, Kraus B, Hernandez Bort JA 2022. Assessment of the percentage of full recombinant adeno-associated virus particles in a gene therapy drug using CryoTEM. PloS one 17(6):e0269139.
27. De Sá Magalhães S, De Santis E, Hussein-Gore S, Colomb-Delsuc M, Keshavarz-Moore E 2022. Quality assessment of virus-like particle: A new transmission electron microscopy approach. Frontiers in Molecular Biosciences 9.
28. Chelius D, Hühmer AF, Shieh CH, Lehmberg E, Traina JA, Slattery TK, Pungor E 2002. Analysis of the adenovirus type 5 proteome by liquid chromatography and tandem mass spectrometry methods. Journal of proteome research 1(6):501-513.
29. van Tricht E, de Raadt P, Verwilligen A, Schenning M, Backus H, Germano M, Somsen GW, Sänger-van de Griend CE 2018. Fast, selective and quantitative protein profiling of adenovirus-vector based vaccines by ultra-performance liquid chromatography. Journal of Chromatography A 1581:25-32.
30. Kulanayake S, Tikoo SK 2021. Adenovirus Core Proteins: Structure and Function. Viruses 13(3).

Journal Pre-proof

Adenovirus Protein (Variants)	Location	Function	Undergoes cleavage
L1 52/55k	Inside the empty capsid (non-structural protein)	• Assembly of infectious particle[11] • Encapsidation of viral DNA	✓
Mu, X	Inside the capsid (core protein)	• Condenses Adenovirus genome • Alters accumulation of E2 proteins • Is involved in increasing DNA transfection efficiency[30]	✓
Protease, AVP	Inside the empty capsid (core protein)	• Essential for virus maturation • Production of infectious progeny • Cleavage of precursors IIIa, VI, VIII, Mu, TP, L1 52/55k[30]	
Protein II, Hexon	Capsid	• Major coat protein • Hexon coat proteins are synthesised during late infection and form homo-trimers	
Protein III, Fiber Protein, Penton Base	Capsid	• Major capsid protein that self-associates to form penton base pentamers • Involved in virus secondary attachment to host cell after initial attachment by the fiber protein, and in endocytosis of virions • As the virus enters the host cell, penton proteins are shed.	
Protein IIIa	Minor Capsid	• Interacts with L1 52/55K to help with the encapsidation of the viral DNA	✓
Protein V	Core protein	• Associates with the viral genome and bridges the core and the capsid proteins • Appears to be essential for virus replication in primary cells[30]	
Protein VI (VI(1), VI(2), VI(3))	Minor Capsid	• It functions as a cofactor for the adenovirus protease (AVP) • As a chaperone for nuclear transport • Essential for virus assembly and endosome lysis	✓
Protein VII (VII(1), VII(2), VII(3))	Core protein	• Nuclear transport of the viral genome acts as cellular histone[30]	✓

Journal Pre-proof

Protein VIII (VIII(1), VIII(2), VIII(3))	Minor Capsid	• Structural component of the virion that acts as a cement protein on the capsid interior and which connect the peripentonal hexons and group-of-nine hexons together	✓
Protein IX	Minor Capsid	• Most flexible molecule among the cement proteins. • Acts as a transcriptional activator of Ad genes • Reorganize host cell nuclear domains.	

Table 1. Key adenoviral structural proteins and their functional characteristics.[30]

Sample	**TEM analysis**			**Virus Particle Analysis**		
	Complete Particles	Incomplete Particles	Relative Abundance of Complete particle (%)	Virus particle concentration (VP/mL) – qPCR	Infective particle concentration (VP/mL)	Infectivity Ratio (P:I)
Ad5 CsCl	4185	240	95	4.3×10^{11}	1.2×10^{11}	4
Ad5 AEX	752	238	76	1.2×10^{11}	8.6×10^{09}	14

Table 2. TEM analysis of transmission electron microscopy images of Ad5 samples purified by CsCl ultracentrifugation or anion exchange chromatography.

Sample	**TEM analysis**			**Mass Spectrometry Analysis**		**Virus Particle Analysis**		
	Complete Particles	Incomplete Particles	Complete particle percent (%)	L1 52/55k peak analysis (RA^{α})	L1 52/55k peptide analysis (RA^{β})	Virus particle Conc. (VP/mL) - qPCR	Infective Particle Conc. (VP/mL)	Infectivity Ratio (P:I)

ChAdOx 1st LDF	2291	1400	62	82	5.5	1.0×10^{11}	8.9×10^{08}	113
ChAdOx 2nd LDF	684	843	45	66	5.6	5.6×10^{10}	7.3×10^{08}	77
ChAdOx 1st HDF	3339	266	93	8	2.0	8.5×10^{11}	1.1×10^{10}	79
ChAdOx 2nd HDF	5791	50	99	10	1	3.4×10^{11}	3.4×10^{11}	56

Table 3. Analytical comparison of TEM; LC-MS and virus particle data for ChAdOx1 fractions taken from CsCl ultracentrifugation purification. $^{\alpha}$relative peak abundance determined from RP-UHPLC. $^{\beta}$median relative abundance of L1 52/55k determined from peptide analysis.

Journal Pre-proof